

Synthesis, Structure, and Mössbauer Study of $[\text{Fe}(\text{H}_2\text{O})_2(\text{C}_9\text{O}_6\text{H}_4)] \cdot \text{H}_2\text{O}$: A Two-Dimensional Iron(II) Trimellitate (MIL-67)

Myriam Riou-Cavellec,^{*,†} Cédric Lesaint,[†] Marc Noguès,[†] Jean-Marc Grenèche,[‡] and Gérard Férey^{*,†}

Institut Lavoisier-Franklin FR 2383, (UMR CNRS 8637 and 8634), Université de Versailles St Quentin, 45 Avenue des Etats-Unis, 78035 Versailles Cedex, France, and Laboratoire de Physique de l'Etat Condensé (UMR CNRS 6087), Université du Maine, Avenue O. Messiaen, 72085 Le Mans Cedex 9, France

Received December 13, 2002

The two-dimensional (2D) iron trimellitate $[\text{Fe}(\text{H}_2\text{O})_2(\text{C}_9\text{O}_6\text{H}_4)] \cdot \text{H}_2\text{O}$, labeled MIL-67, has been obtained under hydrothermal conditions (473 K, 48 h). In the 2D structure of MIL-67, the Fe^{2+} ions display two different octahedral environments: $[\text{FeO}_4(\text{H}_2\text{O})_2]$ and $[\text{FeO}_2(\text{H}_2\text{O})_4]$. These octahedra share an apical water molecule to form infinite chains. The chains are linked by partly deprotonated $\text{C}_9\text{O}_6\text{H}_4^{2-}$ anions to give hybrid organic–inorganic layers; the remaining acidic $-\text{CO}_2\text{H}$ group is dangling in the interlayer space. Below 8(1) K, MIL-67 displays a canted antiferromagnetic behavior, according to analyses via magnetic measurements and Mössbauer spectroscopy. Crystal data for MIL-67 are as follows: triclinic; space group $P\bar{1}$ (No. 2), with $a = 6.9671(2)$ Å, $b = 7.3089(3)$ Å, $c = 12.5097(3)$ Å, $\alpha = 78.758(1)^\circ$, $\beta = 89.542(2)^\circ$, and $\gamma = 65.197(1)^\circ$; volume $V = 565.21(3)$ Å³; and $Z = 2$.

Introduction

The domain of open frameworks currently has undergone tremendous development, because of the numerous applications of open frameworks in catalysis, gas separation, and fine chemicals.¹ In addition to the purely inorganic skeletons, the use of organic moieties for building hybrid organic–inorganic networks is of current interest, because of the variability of the nature of the organic component, which allows an incremental modulation of the size of the frameworks. The main focus was placed on diphosphonates,² polycarboxylates, and pyridylcarboxylates.³ Many interesting results are obtained with rigid polycarboxylates in which the inorganic components are clusters⁴ or chains of octahedra linked either by corners⁵ or edges.⁶

Our main contribution to the knowledge of this type of solid concerns the hydrothermal synthesis of hybrid materials

that contain 3d transition metals (cobalt, vanadium, nickel, iron, chromium), in an attempt to introduce significant magnetic properties in these open-framework structures.

The nature of the metal partially influences the magnetic performances, and, from this point of view, iron could be a good candidate to increase the values of the temperatures of magnetic ordering of such compounds. Several three-dimensional (3D) iron(II) carboxylates have already been obtained with 1,3,5-benzenetricarboxylic (MIL-45)⁷ or 1,2,4,5-

* Authors to whom correspondence should be addressed. E-mail: cavellec@chimie.uvsq.fr; ferey@chimie.uvsq.fr.

[†] Université de Versailles St. Quentin.

[‡] Université du Maine.

- (1) (a) Cheetham, A. K.; Férey, G.; Loiseau T. *Angew. Chem., Int. Ed. Engl.* **1999**, *38*, 3268. (b) Davis, M. E. *Nature* **2002**, *147*, 813. (c) Férey, G. *Chem. Mater.* **2001**, *13*, 3084. (d) Thomas, J. M. *Angew. Chem., Int. Ed. Engl.* **1999**, *38*, 3588. (e) Corma, A. *Chem. Rev.* **1995**, *95*, 559.
- (2) (a) Riou, D.; Baltazar, P.; Férey, G. *Solid State Sci.* **2000**, *2*, 127. (b) Serpaggi, F.; Férey, G. *J. Mater. Chem.* **1998**, *8*, 2749.

- (3) (a) Gutschke, S. O. H.; Molinier, M.; Powell, A. K.; Winpenny, R. E. P.; Wood, P. *Chem. Commun.* **1996**, 823. (b) Serpaggi, F.; Férey, G. *J. Mater. Chem.* **1998**, *8*, 2737. (c) Yaghi, O. M.; Davis, C. E.; Li, G.; Li, H. *J. Am. Chem. Soc.* **1997**, *119*, 2861. (d) Li, H.; Eddaoudi, M.; O'Keeffe, M.; Yaghi, O. M. *Nature* **1999**, *402*, 276. (e) Huang, Z.-L.; Drillon, M.; Masciocchi, N.; Sironi, A.; Zhao, J.-T.; Rabu, P.; Panissod, P. *Chem. Mater.* **2000**, *12*, 2805. (f) Kongshaug, K. O.; Fjellvag, H. *Solid State Sci.* **2002**, *4*, 443. (g) Livage, C.; Guillo, N.; Marrot, J.; Férey, G. *Chem. Mater.* **2001**, *13*, 4387. (h) Lu, J. Y.; Babb, A. M. *Chem. Commun.* **2002**, 1340.
- (4) (a) Eddaoudi, M.; Kim, J.; Rosi, N.; Vodak, D.; Wachter, J.; O'Keeffe, M.; Yaghi, O. M. *Science* **2002**, *295*, 469. (b) Chui, S. S.-Y.; Lo, S. M.-F.; Charmant, J. P. H.; Orpen, A. G.; Williams, I. D. *Science* **1999**, *283*, 1148.
- (5) (a) Barthelet, K.; Marrot, J.; Riou, D.; Férey, G. *Angew. Chem., Int. Ed.* **2002**, *41*, 281. (b) Serre, C.; Millange, F.; Thouvenot, C.; Noguès, M.; Marsolier, G.; Louër, D.; Férey, G. *J. Am. Chem. Soc.* **2002**, *124*, 13519.
- (6) Sanselme, M.; Grenèche, J. M.; Riou-Cavellec, M.; Férey, G. *Chem. Commun.* **2002**, *18*, 2172.
- (7) Riou-Cavellec, M.; Albinet, C.; Livage, C.; Guillo, N.; Noguès, M.; Grenèche, J.-M.; Férey, G. *Solid State Sci.* **2002**, *4*, 267.

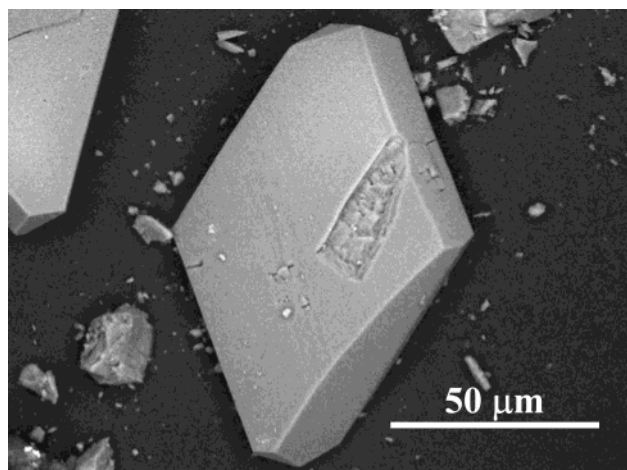


Figure 1. SEM photograph of a crystal of MIL-67.

benzenetetracarboxylic acids (MIL-62⁶ and 66⁸). Therefore, we have extended our investigations to the 1,2,4-benzenetricarboxylic moiety. With this latter development, a single bidimensional compound—[Fe(H₂O)₂(C₉O₆H₄)]·H₂O, labeled MIL-67—was obtained. This paper describes its synthesis, its layered structure, and the ⁵⁷Fe Mössbauer results in the paramagnetic and magnetic ranges.

Experimental Section

Synthesis and Physicochemical Characterizations. The title compound [Fe(H₂O)₂(C₉O₆H₄)]·H₂O, or MIL-67, was hydrothermally synthesized (under autogenous pressure) from a mixture of iron powder (99%+; Riedel de Haën), 1,2,4-benzenetricarboxylic (or trimellitic) acid (C₉O₆H₆, 99%+; Aldrich), and water in the molar ratio of 1:1.5:200 (5 mL). Reactants were introduced in a 23-mL polytetrafluoroethane (PTFE)-lined stainless-steel acid-digestion bomb (initial pH of 1) and heated at 473 K for 2 days (final pH of 1). The resulting solid was filtered, washed with distilled water, and dried at room temperature; the resulting solid was pure and MIL-67 crystallized as colorless lozenge crystals (Figure 1).

Elemental analysis results for MIL-67 are as follows: Fe, 16.36% (Calc., 17.56%); C, 33.76% (Calc., 33.96%). The density (1.90(4) g/cm³, as measured with a Accupyc 1330 pycnometer) is in agreement with the theoretical value (1.87 g/cm³, calculated).

Thermogravimetric analysis (TGA) experiments performed under an O₂ gas flow (on a Perkin–Elmer model TGA-7DX device, at a heating rate of 5 K/min) shows two distinct weight losses (Figure 2). The first weight-loss event, which occurs at 413 K, corresponds to the departure of both nonbonded and coordinated water molecules (Exp., ~16.66%; Calc., 16.98%). This activity involved the collapse of the structure. The subsequent loss involves the calcination of the organic moiety at ca. 613 K (Exp. ≈ 56.9%). At 1073 K, the final residue was identified via X-ray diffractometry (XRD) as α-Fe₂O₃ and the expected total weight loss (74.83%) is in good agreement with the observed weight loss (73.56%).

The infrared spectrum of MIL-67 indicated that both –CO₂[–] and –CO₂H complexes are observed in the title compound, with vibrational bands at ~1616 and 1585 cm^{–1} for carboxylates and at ~1230–1264 and 1703 cm^{–1} for the carboxylic group. The large band at 3422 cm^{–1} originates both from water –OH stretching vibrations and from the dangling carboxylic group.

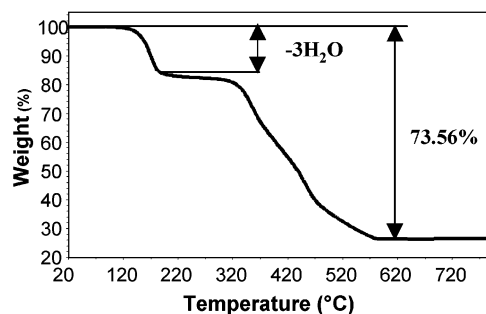


Figure 2. TGA curve of MIL-67 under an O₂ gas flow.

All the characterization results are in agreement with the structural determination.

Magnetization Measurements and ⁵⁷Fe Mössbauer Spectrometry. The magnetization of MIL-67 was measured with a SQUID magnetometer. The *M*(*T*) values were measured under applied magnetic fields of 0.5 and 0.01 T and the *M*(*H*) value was determined for *H* = 0–5.5 T.

Mössbauer experiments were conducted at 300, 77, and 4.2 K by means of a bath cryostat, using a constant acceleration spectrometer and a ⁵⁷Co source that was diffused into a rhodium matrix. The values of the isomer shift (IS) are quoted relative to that of α-Fe foil at 300 K. The hyperfine parameters were refined using a least-squares fitting procedure in the MOSFIT program.⁹

Structure Determination. The microscope was used to select a suitable single crystal (0.108 mm × 0.070 mm × 0.040 mm), and the selected crystal was glued on a glass fiber. The XRD data were collected on a Siemens SMART diffractometer that was equipped with a charge-coupled device (CCD) bidimensional detector ($\lambda_{\text{Mo-K}\alpha} = 0.71073 \text{ \AA}$, 60 s per frame). After reduction, data were corrected from absorption by applying the SADABS program¹⁰ (3913 reflections collected, 2773 unique reflections, $R_{\text{int}} = 0.0167$). The structure of MIL-67 was solved by direct methods (using the TREF option) in the centrosymmetric space group *P* $\bar{1}$ (No. 2) and refined using the SHELX-TL software package.¹¹ Fe (which was located on two half-multiplicity sites) and some coordinated O atoms were located initially, and the remaining O and C atoms were deduced from Fourier-difference maps. H atoms of the CH groups of the aromatic ring were located by applying geometrical constraints (HFIX 43), whereas those that belonged to the coordinated O(2)^w and O(4)^w water molecules (H2aw and H2bw, and H4aw and H4bw, respectively, Table 2) were located without any constraint from Fourier-difference calculations. The positions of all non-hydrogen atoms were refined anisotropically. After the refinement cycles, reliability factors were $R_1(F) = 0.0370$ and $wR_2(F^2) = 0.0976$ for 2335 reflections with $I > 2\sigma(I)$, 192 refined parameters.

The conditions of data collection are summarized in Table 1, whereas the atomic coordinates and principal bond lengths and angles are given in Tables 2 and 3.

Results and Discussion

MIL-67 exhibits a two-dimensional (2D) structure that is built up from hybrid organic–inorganic layers (Figure 3) stacked along the [001] direction. A layer results from the connection of inorganic chains by C₉O₆H₄^{2–} organic moieties

(9) Teillet, J.; Varret, F., MOSFIT Program; unpublished work.

(10) Sheldrick, G.; SADABS Program: Siemens Area Detector Absorption Corrections; unpublished work.

(11) Sheldrick, G.; SHELX-TL software package (including SAINT program); University of Göttingen: Göttingen, Germany, 1994.

(8) Sanselme, M; Riou-Cavellec, M; Férey, G. *Solid State Sci.* **2002**, *11–12*, 1419.

Table 1. Crystal Data and Structure Refinement for MIL-67

formula	$[Fe(H_2O)_2(C_9O_6H_4)] \cdot H_2O$
fw	318.02 g/mol
temp	293(2) K
cryst syst	triclinic
space group	$P\bar{1}$ (No. 2)
unit-cell dimensions	
<i>a</i>	6.9671(2) Å
<i>b</i>	7.3089(3) Å
<i>c</i>	12.5097(3) Å
α	78.758(1)°
β	89.542(2)°
γ	65.197(1)°
vol	565.21(3) Å ³
Z	2
abs coeff	13.77 cm ⁻¹
reflns collected	3913
independent reflns	2773 [R(int) = 0.0167]
data/restraints/params	2773/0/192
Final R indices [<i>I</i> > 2σ(<i>I</i>)]	R ₁ (F) = 0.0370, wR ₂ (F ²) = 0.0976
R indices (all data)	R ₁ (F) = 0.0457, wR ₂ (F ²) = 0.1045
largest diff. peak and hole	0.599 and -0.451 e/Å ³

Table 2. Atomic Coordinates and Equivalent Isotropic Displacement Parameter ($U(eq)$)^a for MIL-67

	atomic coordinate ($\times 10^{-4}$)			$U(eq)$ ($\times 10^3 \text{ \AA}^2$)
	<i>x</i>	<i>y</i>	<i>z</i>	
Fe(1)	0	5000	0	18(1)
Fe(2)	-5000	0	0	20(1)
O(1)	-2052(3)	4224(2)	1033(1)	24(1)
O(2) ^w	-5322(3)	7836(3)	1277(2)	32(1)
H(2AW)	-545(5) ^b	804(5) ^b	184(3) ^b	43(10)
H(2BW)	-445(7) ^b	662(7) ^b	128(4) ^b	68(13)
O(3)	2045(2)	4196(3)	1446(1)	26(1)
O(4) ^w	-1534(3)	8266(3)	232(2)	25(1)
H(4AW)	-100(5) ^b	879(5) ^b	-33(3) ^b	45(9)
H(4BW)	-110(6) ^b	845(6) ^b	84(3) ^b	55(11)
O(5)	-4897(3)	1907(3)	994(1)	29(1)
O(6)	2271(3)	2847(4)	5590(2)	46(1)
O(7)	5298(4)	2074(4)	6561(2)	55(1)
O(8)	-81(3)	839(3)	1558(2)	41(1)
C(1)	5145(3)	2833(3)	2677(2)	20(1)
C(2)	4003(3)	2998(3)	1624(2)	20(1)
C(3)	4153(4)	2876(3)	3642(2)	22(1)
H(3)	2731(4) ^b	3119(3) ^b	3629(2) ^b	27
C(4)	7289(3)	2500(3)	2702(2)	21(1)
C(5)	8376(4)	2236(4)	3691(2)	31(1)
H(5)	9787(4) ^b	2031(4) ^b	3707(2) ^b	38
C(6)	5269(4)	2559(4)	4636(2)	27(1)
C(7)	-1550(3)	2500(3)	1679(2)	23(1)
C(8)	7364(4)	2276(4)	4651(2)	32(1)
H(8)	8094(4) ^b	2112(4) ^b	5308(2) ^b	38
C(9)	4287(4)	2473(4)	5695(2)	33(1)
OW	-228(4)	-2726(3)	2614(2)	49(1) ^a

^a $U(eq)$ is defined as one-third of the trace of the orthogonalized U_{ij} tensor. ^b For H atoms, the atomic coordinate is expressed in units of $\times 10^{-3}$.

(Figure 4a). Chains of corner-sharing Fe^{2+} octahedra are based on two different types of alternated octahedra, $[Fe(1)O_4(H_2O)_2]$ and $[Fe(2)O_2(H_2O)_4]$, with the shared vertex being, in fact, occupied by the water molecule $O(4)^w$ (Figure 4). This is quite unusual, but the various H atoms were easily located and previous chemical characterizations agreed with the presence of this apical water molecule. Moreover, bond lengths within these octahedra (Table 3) indicate that $Fe(1)-O$ bond distance varies over a range of 2.098–2.138 Å, whereas the $Fe(1)-O(4)^w$ bond is significantly longer (2.247 Å). The same feature also concerns the $Fe(2)$ atom: the usual bond distances are 2.062 Å for $Fe(2)-O$ and 2.100 Å for $Fe(2)-O(2)^w$ (with $O(2)^w$ being a terminal water

Table 3. Bond Lengths and Angles for MIL-67

Bond Lengths (Å)			
$Fe(1)-O(1)$	$2.098(2) \times 2$	$Fe(2)-O(5)$	$2.062(2) \times 2$
$Fe(1)-O(3)$	$2.138(2) \times 2$	$Fe(2)-O(2)^w$	$2.100(2) \times 2$
$Fe(1)-O(4)^w$	$2.247(2) \times 2$	$Fe(2)-O(4)^w$	$2.196(2) \times 2$
Bond Lengths within 1,2,4-Benzenetricarboxylate ^a (Å)			
$O(3)-C(2)$	1.266(3)	$C(5)-C(8)$	1.387(4)
$O(5)-C(2)$	1.252(3)	$C(8)-H(8)$	0.93
$C(2)-C(1)$	1.503(3)	$C(8)-C(6)$	1.385(4)
$C(1)-C(4)$	1.409(3)	$C(6)-C(9)$	1.489(3)
$C(4)-C(7)$	1.508(3)	$C(9)-O(6)$	1.315(4)
$C(7)-O(1)$	1.265(3)	$C(9)-O(7)$	1.213(3)
$C(7)-O(8)$	1.253(3)	$C(6)-C(3)$	1.398(3)
$C(4)-C(5)$	1.393(3)	$C(3)-H(3)$	0.93
$C(5)-H(5)$	0.93	$C(1)-C(3)$	1.385(3)
Bond Angles within 1,2,4-Benzenetricarboxylate ^a (deg)			
$O(5)-C(2)-O(3)$			125.6(2)
$O(8)-C(7)-O(1)$			124.5(2)
$O(7)-C(9)-O(6)$			124.7(2)

^a See Figure 4c.

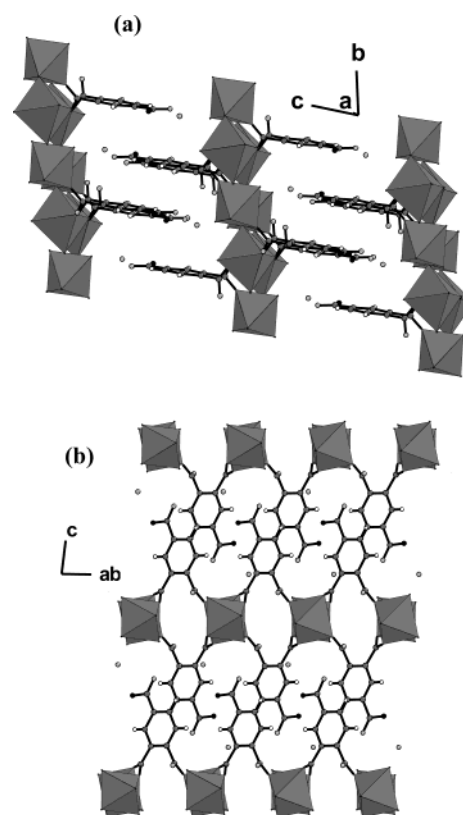


Figure 3. (a) Two-dimensional structure of MIL-67 with a dangle carboxylic complex in the interlayer space; layers are stacked along the [001] direction. (b) A layer is built up from the connection of inorganic chains by trimellitate moieties.

molecule), whereas a longer bond involving the bridging $O(4)^w$ water molecule is observed ($Fe(2)-O(4)^w = 2.196$ Å). Bond valence analysis¹² confirmed that (i) iron is at the expected oxidation state, which is +2 (1.920 v.u. for $Fe(1)$ and 2.142 v.u. for $Fe(2)$), and (ii) $O(4)^w$, which receives 0.25 and 0.29 v.u. from the two Fe atoms, is actually a water molecule. However, given the Mössbauer results and the sign of the electric-field gradients (EFGs) described below, one

(12) Brese, N. E.; O'Keeffe, M. *Acta Crystallogr. Sect. B: Struct. Sci.* **1991**, *B47*, 192.

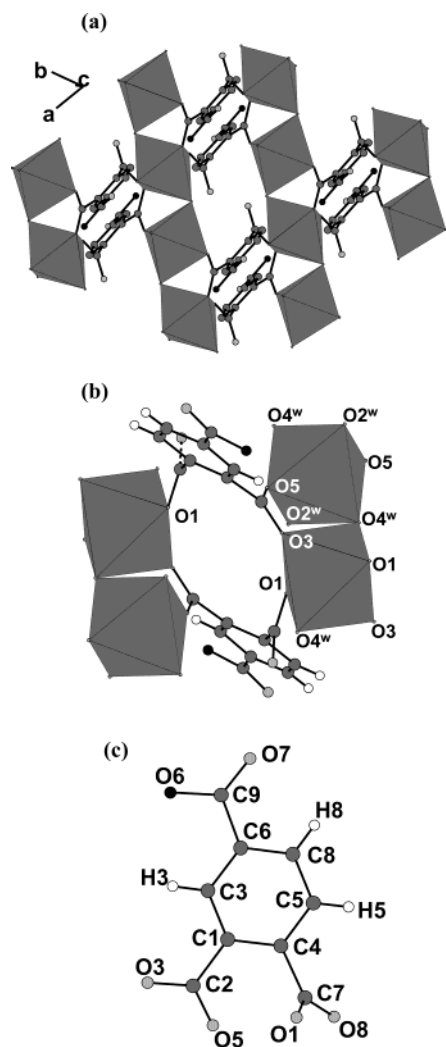


Figure 4. (a) Within a layer, chains are oriented along the $[1\bar{1}0]$ direction. (b) Connection of two neighboring chains by carboxylates; the acidic O(6) atom is black. (c) Atom labels within the 1,2,4-benzenetricarboxylate moiety.

must consider the two iron octahedra and their distortion in another way, according to the major species that are bound to the Fe^{2+} atom. Indeed, around the Fe(1) site, the four O atoms are the main actors of the coordination ($\langle d_{\text{Fe}(1)-\text{O}} \rangle = 2.118 \text{ \AA}$), in terms of bond valence, and the two water molecules are just affixed to the Fe(1) site but at a longer distance, to ensure the electrostatic balance. For this reason, the Fe(1) octahedron may be considered to be elongated. In contrast, four water molecules ($\langle d_{\text{Fe}(2)-\text{O}} \rangle = 2.148 \text{ \AA}$) surround the Fe(2) site with weak bonds and the electrostatic balance can be attained using two oxygen O(5) atoms that are strongly bonded to the Fe(2) site (where the Fe(2)–O(5) bond distance is 2.062 \AA). Therefore, this time, the Fe(2) octahedron is flattened. These two antagonistic features are illustrated during the Mössbauer study by very different EFGs (see below).

The connection of the inorganic chains is then ensured by the organic tricarboxylates in such a way that the carboxylate group C(2)/O(3)/O(5) bridges two consecutive octahedra of a single chain. The second carboxylate group, C(7)/O(1)/O(8), connects with a neighboring chain via the O(1) atom (see Figures 4 and 3b), where the O(8) atom

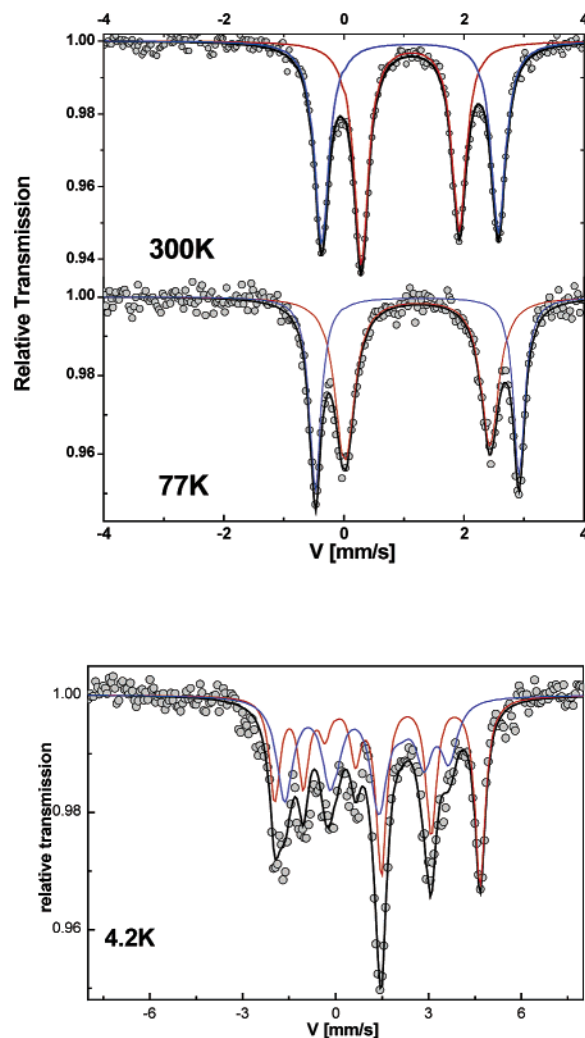


Figure 5. Mössbauer spectra of MIL-67 recorded at 300, 77, and 4.2 K.

remains noncoordinated. The third group, C(9)/O(6)/O(7), is a carboxylic complex in which the O(6) atom is the acidic oxygen, in agreement with the observed C(9)–O(6) bond length (1.315 \AA ; see Table 3); it is dangling in the interlayer space. The free O^{w} water molecule is not located far from this dangling function ($\text{O}(6)–\text{O}^{\text{w}} = 2.655 \text{ \AA}$) and develops hydrogen bonds with the acidic O(6)–H group. Finally, the torsion of the trimellitate species is also noticeable; although the carboxylic complex remains in the aromatic ring plane, both bonding carboxylate groups are strongly deviated from this latter determination (the torsion angles are 70° for the monodentate C(7)/O(1)/O(8) and 34° for the bridging bidentate C(2)/O(3)/O(5)).

The Mössbauer spectra of MIL-67, recorded at 300 and 77 K (Figure 5), exhibit two doublets, which are well reproduced using two quadrupolar components without any constraints. The theoretical expected proportion for each component is 50% for the Fe(1) octahedron and 50% for the Fe(2) octahedron, according to the crystallographic data. The obtained refined parameters are listed in Table 4, and their proportions are in good agreement with the expected ones, thus excluding the possible presence of any impurities in the sample. Moreover, the two IS values are consistent with high-spin-state Fe^{2+} ions in octahedral coordination; the

Table 4. Refined Values of Hyperfine Parameters at 77 and 300 K

temp, T (K)	component, Γ_i	isomer shift, IS ^a (mm/s)	linewidth at half height, FWHM ^a (mm/s)	quadrupolar splitting, QS ^a (mm/s)	ratio of each component ^b (%)
300	Γ_1	1.22	0.29	1.63	51
	Γ_2	1.24	0.29	2.91	49
77	Γ_1	1.35	0.36	2.40	55
	Γ_2	1.36	0.23	3.36	45 ^a

^a Standard deviation = ± 0.02 mm/s. ^b Standard deviation = $\pm 5\%$.

Table 5. Refined Values of Hyperfine Parameters at 4.2 K

isomer shift, IS ^a (mm/s)	linewidth at half height, FWHM ^a (mm/s)	quadrupolar splitting, QS ^a (mm/s)	hyperfine field, B_{hyp}^b (T)	asymmetry parameter, η^c	polar angle (deg) ^d			ratio of each component ^e (%)
					ϑ	γ	β^f	
1.32	0.64	-2.05	12.9	0.9	52	0	-39	47
1.33	0.41	3.33	13.7	1.0	55	13	38	53 ^a

^a Standard deviation = ± 0.02 mm/s. ^b Standard deviation = ± 0.5 T. ^c Standard deviation = ± 0.1 . ^d The polar angles ϑ and γ are defined by the direction of the hyperfine field in the EFG coordinate system. Standard deviation = $\pm 5^\circ$. ^e β is the angle defined by the direction of the hyperfine field, relative to the γ -beam. ^f Standard deviation = $\pm 5\%$.

thermal evolution of quadrupolar splitting (QS) is also characteristic of iron at the divalent oxidation state (+2). It is important to stress that the line widths differ for both quadrupolar doublets at 77 K, whereas these values remain similar at 300 K, as illustrated in Figure 5. In addition, one observes a slight asymmetry of quadrupolar doublets, which is due to texture, the presence of which has been checked by rotating the sample, with respect to the γ -radiation.¹³ This preferential orientation might be favored by the presence of a layered structure, despite the powdered nature of the sample.

At low temperature, the quadrupolar hyperfine structure splits into a magnetic hyperfine structure, revealing unambiguously a long-range magnetic order. The 4.2-K Mössbauer spectrum (see Figure 5 and Table 5) can be described by means of two rather equiprobable components, both of which exhibit broadened lines. Both the IS and quadrupolar interaction are consistent with those obtained at high temperature and thus confirm the presence of high-spin-state Fe^{2+} ions in octahedral coordination. The high value of the asymmetry parameter, η , which is defined as $(V_{xx} - V_{yy})/V_{zz}$ (assuming $|V_{xx}| \leq |V_{yy}| \leq |V_{zz}|$ to get $0 \leq \eta \leq 1$), suggests a nonaxial EFG tensor that is attributed to highly distorted octahedral Fe units. The positive and negative values of the EFG thus corroborate the two types of distortion with flattened Fe(2) and elongated Fe(1) octahedra. The positive QS values encountered in many iron(II) oxides seem to suggest that the Fe(1) octahedron corresponds to the Γ_2 contribution to the spectrum. In addition, one observes a rather low hyperfine field value, which results from the difference between the Fermi (usually negative), orbital, and dipolar contributions. Note that, in this case, the hyperfine field, typical of divalent iron, is not proportional to the iron magnetization, because of the low EFG symmetry.

Concerning the magnetic behavior of MIL-67, the $\chi^{-1}(T)$ curve (see Figure 6) indicates that MIL-67 fits a paramagnetic Curie–Weiss law at > 100 K: $\chi_{mol}^{-1} = 0.232T + 8.38$. The deduced Curie constant ($C_{mol} = 4.31$) and magnetic moment ($\mu_{exp} = 5.87 \mu_B/mol$) are high for Fe^{2+} (usually, $\mu(Fe^{2+}) =$

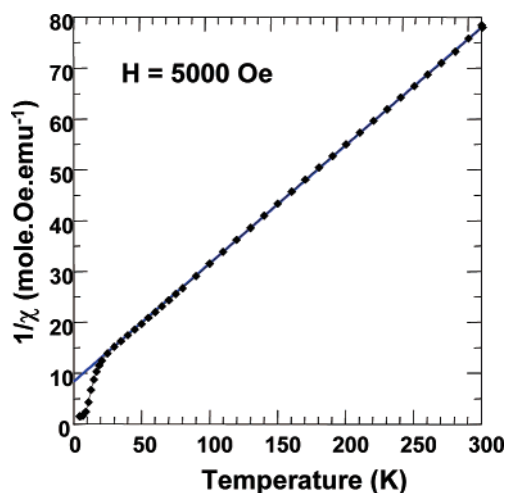


Figure 6. $\chi^{-1}(T)$ curve under a field of $H = 0.5$ T (the straight line is related to the Curie–Weiss law).

$5.4 \mu_B/mol$, taking into account some L–S coupling); however, similar values have already been observed for other iron(II) carboxylates, on the basis of strongly tilted corner-sharing Fe^{2+} octahedra.^{8,14} Below ca. 50 K, $\chi^{-1}(T)$ deviates from the paramagnetic law and a strong increase of magnetization is observed below ca. 8 K (see Figure 7), which is indicative of either ferrimagnetic or canted antiferromagnetic behavior, according to the observed negative Curie–Weiss temperature ($\theta_p = -36$ K). However, the shape of the $\chi^{-1}(T)$ curve at 4.5 K (Figure 8) is typical of a canted antiferromagnet with a fast increase of the resulting magnetization at very low fields and a linear variation of $M(H)$ at $H > 0.5$ T. The extrapolation of the latter to $H = 0$ gives a resulting magnetization of $0.54 \mu_B/mol$ at 4.5 K, which may result from both slightly different magnetizations on the two sites and a small canting of the moments.

Moreover, it is not obvious that, within the layers, the magnetic interactions between the Fe^{2+} cations are of the 180° superexchange type, as long as the $Fe^{2+}-O(4)^w-Fe^{2+}$ angle is $\sim 119.6^\circ$ (this weak value is induced by the geometry of bridging carboxylates, because the $O \cdots O$ distance within a $-CO_2^-$ group is $\sim 2.24 \text{ \AA}$). However, these interactions

(13) Grenèche, J.-M.; Varret, F. *J. Phys. C: Solid State Phys.* **1982**, *15*, 5333.

(14) Riou-Cavellec, M.; Férey, G. *Solid State Sci.* **2002**, *4*, 1221.

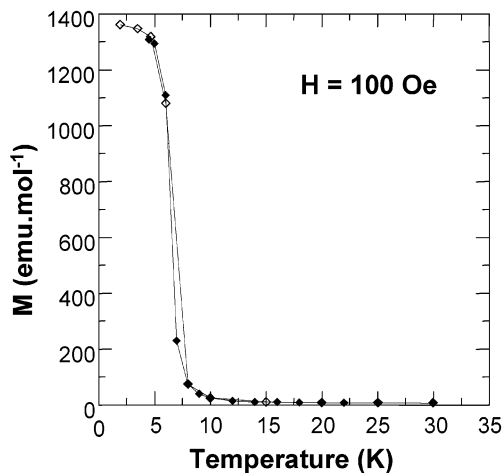


Figure 7. $M(T)$ curve under a field of $H = 0.01$ T, showing an increase below 8(1) K.

are mainly antiferromagnetic, according to the observed negative θ_p value and to Goodenough's orbital overlap theory.¹⁵ Finally, the 3D magnetic order originates from dipolar interactions.

Conclusion

The two-dimensional iron trimellitate $[\text{Fe}(\text{H}_2\text{O})_2(\text{C}_9\text{O}_6\text{H}_4) \cdot \text{H}_2\text{O}]$, or MIL-67, is a new example of a hybrid solid with magnetic properties. The nonsymmetrical position of the

(15) Goodenough, J. B. In *Magnetism and the Chemical Bond*; Interscience: New York, 1963.

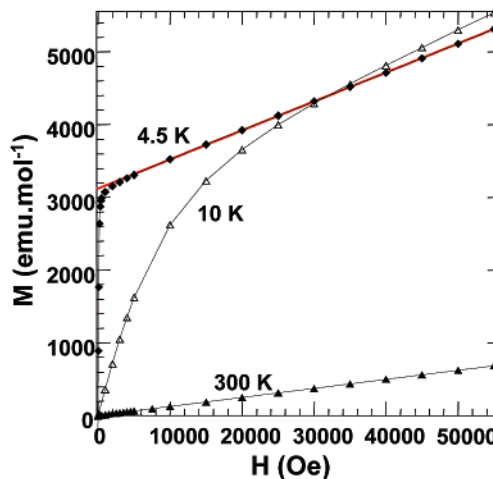


Figure 8. $M(H)$ curves showing the resulting magnetization at 4.5 K.

carboxylate complexes leads to a layered structure with dangling $-\text{CO}_2\text{H}$ groups that point toward the interlayer space and yield hydrogen bonds with the inserted water, ensuring the stability of the structure. The two different environments of the Fe^{2+} ions lead to canted antiferromagnetism at <8 K, according to analysis via magnetic measurements and Mössbauer spectroscopy.

Supporting Information Available: Tables listing complete crystallographic data, anisotropic displacement parameters, and full bond lengths and angles for MIL-67 (CIF). This material is available free of charge via the Internet at <http://pubs.acs.org>.

IC020715Y